Zebrafish *vps33b*, an ortholog of the gene responsible for human arthrogryposis-renal dysfunction-cholestasis syndrome, regulates biliary development downstream of the onecut transcription factor *hnf6*

Randolph P. Matthews[1], Nicolas Plumb-Rudewiez[2], Kristin Lorent[3], Paul Gissen[4], Colin A. Johnson[4], Frederic Lemaigre[2] and Michael Pack[3,5,*]

[1]Division of Gastroenterology and Nutrition, The Children's Hospital of Philadelphia and Department of Pediatrics, University of Pennsylvania School of Medicine, Philadelphia, PA 19104, USA
[2]Hormone and Metabolic Research Unit, University of Louvain Medical School and International Institute of Cellular and Molecular Pathology, Brussels B1200, Belgium
[3]Department of Medicine, University of Pennsylvania School of Medicine, Philadelphia, PA 19104, USA
[4]Section of Medical and Molecular Genetics, University of Birmingham, Birmingham B15 2TT, UK
[5]Department of Cell and Developmental Biology, University of Pennsylvania School of Medicine, Philadelphia, PA 19104, USA
*Author for correspondence (e-mail: mpack@mail.med.upenn.edu)

Accepted 3 October 2005

Development 132, 5295-5306
Published by The Company of Biologists 2005
doi:10.1242/dev.02140

Summary

Arthrogryposis-renal dysfunction-cholestasis syndrome (ARC) is a rare cause of cholestasis in infants. Causative mutations in *VPS33B*, a gene that encodes a Class C vacuolar sorting protein, have recently been reported in individuals with ARC. We have identified a zebrafish *vps33b*-ortholog that is expressed in developing liver and intestine. Knockdown of *vps33b* causes bile duct paucity and impairs intestinal lipid absorption, thus phenocopying digestive defects characteristic of ARC. By contrast, neither motor axon nor kidney epithelial defects typically seen in ARC could be identified in *vps33b*-deficient larvae. Biliary defects in *vps33b*-deficient zebrafish larvae closely resemble the bile duct paucity associated with knockdown of the onecut transcription factor *hnf6*. Consistent with this, reduced *vps33b* expression was evident in *hnf6*-deficient larvae and in larvae with mutation of *vhnf1*, a downstream target of *hnf6*. Zebrafish *vhnf1*, but not *hnf6*, increases *vps33b* expression in zebrafish embryos and in mammalian liver cells. Electrophoretic mobility shift assays suggest that this regulation occurs through direct binding of vHnf1 to the *vps33b* promoter. These findings identify *vps33b* as a novel downstream target gene of the *hnf6/vhnf1* pathway that regulates bile duct development in zebrafish. Furthermore, they show that tissue-specific roles for genes that regulate trafficking of intracellular proteins have been modified during vertebrate evolution.

Key words: Zebrafish, Arthrogryposis-renal dysfunction-cholestasis syndrome, Human, Disease, *tcf2*, *onecut1*

Introduction

The mammalian biliary system transports bile from the liver to the gallbladder and intestine. The intrahepatic biliary system consists of branching ducts arranged in a tree-like configuration that arise at the hepatocyte canaliculus, the site of bile secretion. Heritable syndromes associated with intrahepatic cholestasis, or reduced bile flow, may be associated with one of two types of histologically defined defects of the intralobular bile ducts. Individuals with bile duct paucity have reduced numbers of intralobular bile ducts, whereas in individuals with ductal plate malformation, bile duct development is arrested, presumably as a result of defective biliary remodeling (Kamath and Piccoli, 2003; Johnson et al., 2003).

Mutations in the vacuolar sorting protein VPS33B have been found in individuals with the arthrogryposis-renal dysfunction-cholestasis syndrome (ARC), a rare autosomal recessive disorder (Gissen et al., 2004) associated with joint contractures, altered kidney function and cholestasis. Dysmorphic facial features, diarrhea and poor growth are also common in such individuals (Eastham et al., 2001). Yeast *vps33*, and other class C yeast vacuolar sorting proteins (Vps11, Vps16 and Vps18), play an essential role in intracellular trafficking (Sato et al., 2000; Peterson and Emr, 2001). Mammalian Class C VPS proteins have a similar subcellular localization as their yeast orthologs and are thought to play related roles (Huizing et al., 2001; Kim et al., 2003). Consistent with this idea, mis-sorted liver and kidney membrane proteins have been reported in the pathological specimens from individuals with ARC (Gissen et al., 2004).

Here, we present data showing that knockdown of zebrafish *vps33b* causes cholestasis, bile duct paucity and other defects compatible with a partial ARC syndrome phenocopy. Ultrastructural analysis identifies cytoplasmic inclusions in

biliary and intestinal epithelial cells that resemble those seen in yeast vps class C mutants. These findings suggest that intracellular trafficking is altered in *vps33b*-deficient cells and that the cholestasis, diarrhea and growth retardation seen in individuals with ARC may arise autonomously. By contrast, reduced motor neuron density, which probably accounts for the arthrogryposis in individuals with ARC (Di Rocco et al., 1990), was not evident in *vps33b*-deficient embryos.

Biliary defects in *vps33b*-deficient larvae closely resembled defects associated with knockdown of the onecut family transcription factor *hnf6* (*onecut1* – Zebrafish Information Network) (Matthews et al., 2004). Molecular analyses showed that *vps33b* expression is reduced by knockdown of *hnf6* and by mutation of *vhnf1* (*tcf2* – Zebrafish Information Network) a gene that functions downstream of *hnf6* in zebrafish (Matthews et al., 2004) and mammals (Clotman et al., 2002). Forced expression of *vhnf1* activated *vps33b* expression. Further, vHnf1 protein could bind and activate the *vps33b* promoter. These data show that *hnf6* indirectly regulates *vps33b* expression through its downstream target gene, *vhnf1,* and thus identify a novel pathway active during zebrafish biliary development.

Materials and methods

Isolation of zebrafish vps33b

Full-length *vps33b* cDNA was amplified from zebrafish liver using primers derived from the zebrafish genome assembly (Zv4) (www.sanger.ac.uk) (see Table 1 for primer sequences, vps33b8, vps33b9). Liver cDNA was synthesized from a pool of adult liver RNA and RNA from whole larvae at 24 hpf, 48 hpf and 5 dpf as described previously (Matthews et al., 2004). The resulting cDNA was sequenced and cloned into the expression vector pCS2(+) using standard protocols.

In situ hybridization

Antisense riboprobes for full-length *vps33b*, *ceruloplasmin* and *vhnf1* genes were synthesized as previously described (Wallace and Pack, 2003). In situ hybridization and tissue sectioning of specimens were also performed as described previously (Matthews et al., 2004).

Morpholino oligonucleotides

Morpholino oligonucleotides (MOs) were designed based on sequences available from the zebrafish genome assembly. Morpholinos were designed to target the 5th and 18th exons, as these are sites of *VPS33B* mutations in individuals with ARC. A translational start site morpholino was also designed (Table 1). For the IE5 and IE18 MOs, 1.5 pg was injected at the one-cell stage, whereas 0.2 pg of the translation initiation MO was used. Higher doses were lethal at early embryonic stages. The same dose of a 4 bp mismatch control IE18 MO was lethal at early embryonic stages. Lower doses had no effect on biliary development. For the complementation experiments, the IE18 MO and a previously described *hnf6* MO (Matthews et al., 2004) were used at one-tenth the above amount (150 fg).

To demonstrate specific MO targeting, PCR primers were designed that flanked the 5th exon and the 18th exon (Table 1, vps33b-1, -2, -5 and -6). cDNA synthesized from RNA isolated from 24 hpf control embryos and embryos injected with increasing doses of morpholino was used as template for PCR reactions with these primers. The two distinct products from the IE18-injected embryos were sequenced. The single product from the IE5-injected embryos was also sequenced.

Table 1. Sequences of primers and oligonucleotides

Name	Sequence
vps33b-1	CCGACTTCTCATTGCTCAAAAGAC
vps33b-2	TCTCCATAGACACCCTGTTCCTCC
vps33b-8	GATCTGTCCATATGGCTCAGAC
vps33b-9	TCCTGCGGAATGTTGACTCAAA
vps33b-5	GCAGATGAAGGCGTTTGTTGC
vps33b-6	CTCAGGGGAATGTAAGCACCAC
vps33a-1	TCTTTGTTCGCCCGAGGTTG
vps33a-2	CACCGACAGCATTGAAGTTCTTG
vps33b-11	TGATCCTTGGTGGCTGC
vps33b-12	TGTTGGTGATGGCTGTTGTGAG
vps33b-13	CACTGTTGGTGATGGCTGTTGTG
vps33bp-f2	GAGGGAGGGTTTTTCATATAGAGAGA
vps33bp-r2	TAAACAACTCCTGTCACAATTCTGCTT
MO vps33b-IE5	GAATTAACTAAATCTGTAAAGAAGT
MO vps33b-IE18	CTATACCATAACTCTGAACAAGACA
MO vps33b-ATG	ATCTCTCCTCTCTGTCTGAGCCATA
MO vps33a-ATG	TACCGCAAAACAAATGTGACGCCAT
MO vps33a-EI4	TGCATTTCTACTCACCCGTGCA
vps33b-hnf6-1	ATAGGTAGAAATTGAGTCTATAATAGCTTATAATGC
vps33b-hnf6-2	ATACAGAATATATATGTCACTTATAAATTAAAGAAC
vps33b-hnf6-3	GAACTATTTTTGACCTTATCTATGAATTTTGGTTA-TGGAA
vps33b-vhnf1-1	AGAACTTTATAAAACAGGTTATTATTAAAACACAG-ACAACACT
vps33b-vhnf1-2	GTTTCTCCGCGGCGAAATTAACCGTTTCTAGCAGC-ATG
vps33b-vhnf1-3	TTGCATATGACAACTGTTAAGGCGTAGTTTGCTGAA
vps33b-vhnf1-4	AACGTGTAAATAAAACACTAACCTGAGCTGTATGA

Sequences of primers used for PCR and oligonucleotides used for EMSA are listed.

Morpholinos directed against the translation start site and the splice donor site of exon 4 (EI4) from zebrafish *vps33a* were also designed, based on sequence from the zebrafish genome assembly (Zv4). The sequences of the morpholinos are listed in Table 1. Injection with either *vps33a* morpholino (1.5 pg) produced an identical phenotype. PCR primers to document *vps33a* knockdown are also listed in Table 1 (vps33a-1, -2).

PED-6 treatment

Wild-type (vehicle-injected) and morpholino injected larvae at 5 dpf were soaked overnight in 0.1 μg/ml PED-6; as a control, swallowing function was confirmed using fluorescent beads (Farber et al., 2001; Matthews et al., 2004).

Immunostaining and electron microscopy

Wild-type and morpholino-injected larvae at 3, 4 and 5 dpf were fixed and prepared as described (Matthews et al., 2004). For motor axon staining, 48 hpf larvae were fixed in 4% paraformaldehyde. For electron microscopy, 5 dpf larvae were fixed in buffered gluteraldehyde. Keratin immunostaining of wild-type and morpholino-injected larvae were performed as previously described (Matthews et al., 2004; Lorent et al., 2004). Larvae for motor axon immunostaining were treated with proteinase K and then incubated with mouse anti-ZNP1 and goat anti-mouse Alexa 488-conjugated secondary antibody as described (Lefebvre et al., 2004). Processing and analysis of electron microscopy specimens was identical to previously described methods (Matthews et al., 2004).

For cell proliferation and apoptosis assays, control and IE18-injected larvae were fixed in 4% paraformaldehyde at 3 and 4 dpf. Following collagenase treatment or skin dissection, larvae were incubated in anti-PCNA antibody (Sigma), followed by incubation with HRP-conjugated anti-mouse secondary antibody (Vector Laboratories) and staining using diaminobenzidine. Larvae were then embedded in JB-4, sectioned and examined for nuclear staining in the

liver. For the apoptosis assay, the larvae were assayed using the Apoptag system (Chemicon) sectioned, and assayed for staining in the liver. As a positive control, we pretreated fixed wild-type 4 dpf larvae with 0.1 N HCl, which caused widespread DNA fragmentation.

AM1-43 labeling

Larvae at 5 dpf were soaked in 5 μM AM1-43 (Biotium) overnight and then 30 μM for 1 hour. To remove membrane bound AM1-43, larvae were then washed twice briefly in 10 μM ADVASEP-7, followed by incubation in the ADVASEP-7 for one hour (Kay et al., 1999), at which point they were fixed in 4% paraformaldehyde. The larvae were then embedded in glycol methacrylate and sectioned and examined as described (Wallace and Pack, 2003). For quantification, 200-300 cells per larva from three wild-type and four morpholino-injected larvae were examined, and the ratio of the number of red AM1-43 labeled vesicles to epithelial nuclei was calculated.

Quantitative real-time PCR

cDNA was synthesized from RNA obtained from 3 dpf control and *hnf6* morpholino-injected whole larvae derived from three independent experiments as previously described (Matthews et al., 2004). Additionally, RNA was collected from whole 3 dpf larvae injected with 2 ng/μl *vhnf1* or 20 ng/μl *hnf6* mRNA, as well as from sorted 3 dpf *vhnf1* mutants (Sun and Hopkins, 2001). The resulting cDNA was used as template for real-time quantitative PCR as described previously (Matthews et al., 2004). Primers for *tbp* and *vhnf1* are listed elsewhere (Matthews et al., 2004); the *vps33b* primers are listed in Table 1. Either 3′ primer (12 or 13) was used with the 5′ primer (11). Analysis was performed as described previously (Matthews et al., 2004). For quantification of the PCR bands documenting morpholino efficacy, NIH Image 1.63f was used.

Promoter cloning, transient transfections and luciferase reporter gene assays

A 1.5 kb region of the *vps33b* promoter was cloned from wild-type TLF and AB strain zebrafish embryos using the primers noted in Table 1 (p-f2, p-r2), based on sequence from the zebrafish genome assembly (Zv4). For the transient transfections and gel-shift assays, BMEL cells were cultured as described (Plumb-Rudewiez et al., 2004). For luciferase reporter assays, BMEL cells were transfected using lipofectamine 2000 (Life Technologies), 400 ng pGL-basic-*vps33b*(–1560/+139)-luc, 10 ng of pCS2-*hnf6* or pCS2-*vhnf1* expression vector (Matthews et al., 2004) and 15 ng of the Renilla luciferase coding pRL-SVK3 vector as internal control. Luciferase activities were measured after 24 hours with the dual luciferase assay system in a TD-20/20 luminometer (Promega). Luciferase activities were expressed as the ratio of reporter activity (firefly luciferase) to internal control activity (*Renilla* luciferase).

Electrophoretic mobility shift assays (EMSAs)

For production of vHNF1, HNF6 or GFP, BMEL cells were transfected using lipofectamine 2000 and 25 μg pCS2-*hnf6* or pCS2-*vhnf1* expression vector. Cells were washed with PBS and resuspended in hypertonic buffer, and the nuclear extract was then incubated with ^{32}P-labeled oligonucleotide probe (see Table 1 for sequences). A 50-fold excess of unlabeled probe was added to the binding reaction when testing for binding specificity. Antibodies against HNF1β (vhnf1) (polyclonal sc7411, Santa Cruz) or against HNF1α (polyclonal sc10791, Santa Cruz) were used in supershift experiments. After incubation, the samples were separated by electrophoresis and the gels were exposed.

Results

Identification of a zebrafish *VPS33B* ortholog

A zebrafish *vps33b* candidate gene was identified from genomic sequence using BLAST, and a full-length *vps33b* cDNA was subsequently generated from adult and larval total RNA. Sequence comparison of zebrafish and human *VPS33B* demonstrates an overall 74% amino acid identity with 84% similarity (Fig. 1). Amino acid residues altered by human ARC mutations (Fig. 1) are largely conserved in zebrafish *vps33b*, as are the intron-exon boundaries affected by mutations involved in mRNA processing. Although the precise chromosomal location of zebrafish *vps33b* was not determined, genes in proximity to *vps33b* in the zebrafish genome assembly are located on human chromosome 15q15 and 15q26, the location of human *VPS33B* (Fig. 1). These data strongly suggest that the zebrafish *vps33b* candidate we have identified is orthologous to human *VPS33B*.

Developmental expression of *vps33b*

Human *VPS33B* is expressed in a nearly ubiquitous pattern in adult tissues (Huizing et al., 2001). Staged in situ hybridization in embryonic and larval zebrafish revealed widespread *vps33b* expression at sphere stage (4 hpf) through 24 hpf (Fig. 2). At 48 hpf, *vps33b* expression localized to the brain, retina, ear, liver and proximal intestine. This expression pattern was more pronounced at 72 hpf (Fig. 2) and persisted through 5 dpf (not shown). Close examination of 3 dpf (not shown) and 4 dpf (Fig. 2) larvae revealed a reticular pattern of *vps33b* expression within the liver, suggesting the possibility that *vps33b* is predominantly expressed in the developing biliary epithelial cells. Histological analyses of these specimens, and comparison with larvae that express the hepatocyte gene *ceruloplasmin*, supported this interpretation (Fig. 2). Neither kidney nor spinal cord expression was evident in the whole-mount specimens at any stage analyzed.

vps33b knockdown disrupts zebrafish biliary development

To assay the role of *vps33b* in zebrafish biliary development, gene knockdown experiments using antisense morpholino oligonucleotides were performed. Morpholinos were designed to target the 5′ translational start site and the splice acceptor sites for exons 5 (‘IE5’) and 18 (‘IE18’). These latter sites correspond to regions that contain mutations found in individuals with ARC syndrome (Gissen et al., 2004).

Knockdown of *vps33b* did not affect the overall appearance or liver size of larvae at 5 dpf (Fig. 3A,B). However, gallbladder fluorescence following ingestion of the quenched fluorescent lipid, PED-6, was reduced in *vps33b* morpholino larvae (n=12 of 14 larvae examined; Fig. 3C,D). Transport of this compound to the gallbladder can serve as an indicator of biliary secretion (Farber et al., 2002), biliary morphology (Matthews et al., 2004) and intestinal lipid absorption. Thus, these data suggest the possibility that *vps33b* deficiency might alter biliary development.

Keratin immunohistochemistry of 5 dpf morpholino-injected larvae strongly suggest that altered biliary development contributed to the defects of PED-6 processing. In over 95% of larvae injected with 1.5 pg of the IE5 or IE18 morpholinos, the number of intrahepatic bile ducts was reduced compared with control (n=50 larvae examined; Fig. 3E-J), whereas the extrahepatic biliary tree appeared normal in all morpholino-injected larvae (data not shown). Within the intrahepatic biliary system, defects of the interconnecting and

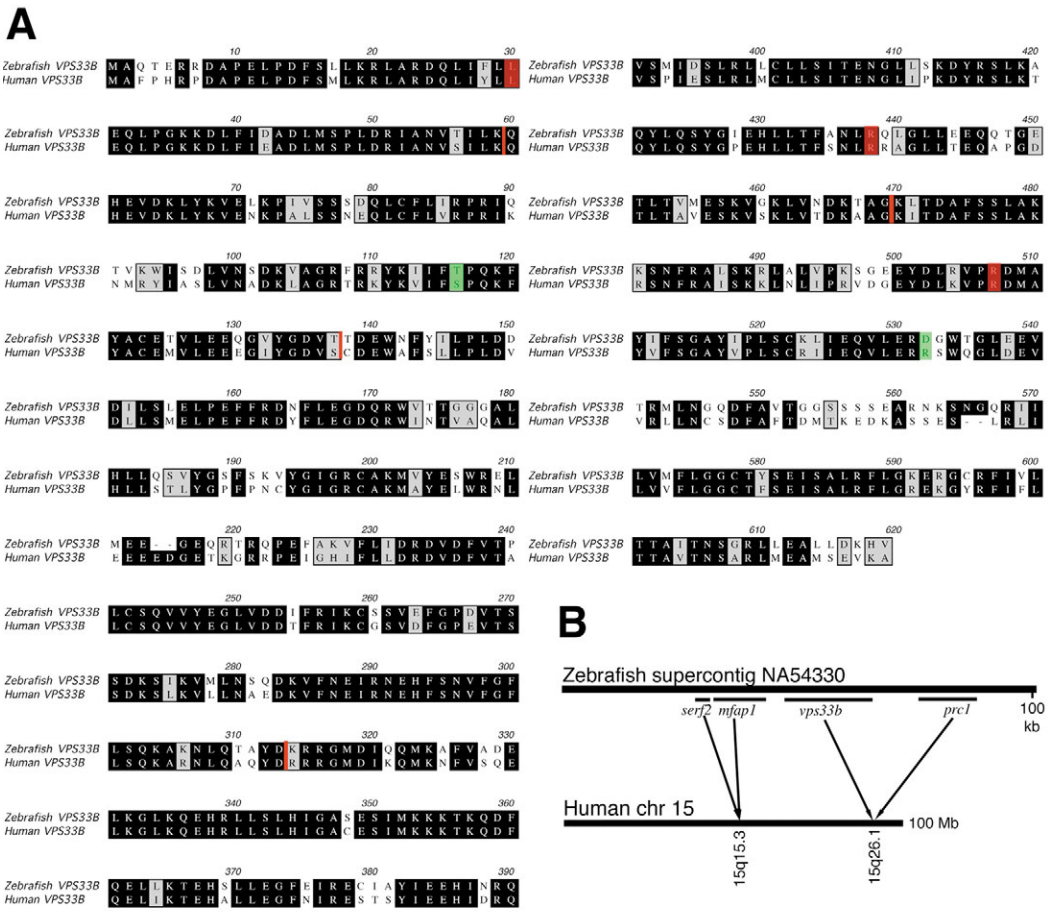

Fig. 1. Sequence and mapping of zebrafish *vps33b*. (A) Deduced amino acid sequence of zebrafish and human *vps33b*. Identical amino acids are shaded black, similar residues in gray. *VPS33B* mutations from individuals with ARC are colored red (identical residue) and green (similar residue). Red lines refer to the location of ARC mutations at splice sites conserved in the zebrafish and human *vps33b*/*VPS33B* genes. (B) Map comparison of zebrafish supercontig NA54330 and human chromosome 15. Supercontig locations of *vps33b* and three other zebrafish genes (*serf2*,small EDRK-rich factor 2; *mfap1*, microfibrillar-associated protein 1; *prc1*, protein regulator of cytokinesis 1) are noted. Arrows indicate locations of the orthologous genes on human chromosome 15.

terminal ducts were most pronounced (Fig. 3H-J and Table 2). Consistent with these selective intrahepatic defects, biliary morphology appeared normal in 3 dpf morpholino-injected larvae, whereas bile duct paucity was evident in 4 dpf larvae and was more pronounced at 5 dpf (see Fig. S1 in the supplementary material), the timepoints when the interconnecting and terminal ducts are first evident (Lorent et al., 2004; Matthews et al., 2004). Importantly, we did not identify alterations of cell proliferation in the developing liver of morpholino-injected larvae, as determined by the percentage of PCNA-positive cells, nor an increased number of cells undergoing apoptosis (Table 3). Taken together, these data support the idea that bile duct paucity in *vps33b* deficiency disrupts either growth of existing biliary epithelial cells or the recruitment of new biliary cells from undifferentiated progenitors.

Molecular analyses of embryos injected with the IE5 and IE18 morpholinos confirmed the targeting of the *vps33b* transcript (Fig. 4). Injection with either morpholino reduced *vps33b* expression, suggesting either decreased stability of the targeted mRNA or interference with an autoregulatory feedback loop. Quantification of the fluorescent intensity of the bands corresponding to the amplified cDNA showed a 30-50% reduction in full-length *vps33b* mRNA in IE18 and IE5 morpholino-injected larvae. Sequencing of cDNA amplified from IE18 morpholino-injected embryos using primers surrounding the targeted exon identified a 15 amino acid in-frame deletion in the predicted sequence encoded by the *vps33b* mRNA. The deleted sequence included nucleotides encoding the conserved arginine (R438) that is mutated to a stop codon in several ARC syndrome kindreds. Although a novel amplification product was not detected in the IE5-injected larvae, these larvae had identical biliary defects as the IE18 morpholino-injected larvae. We hypothesize that the IE5 morpholino leads to splicing at a distant site within the *vps33b* cDNA. Larvae injected with of an eightfold lower dose of a

Table 2. Duct quantification from *vps33b* morpholino-injected 5 dpf larvae

	Long duct (blue) number	Long duct (blue) length	Interconnecting duct (green) number	Terminal ductule (red) number
Control	17±7	6.2±0.7	61±0	107±13
vps33b IE18-injected	14±5	5.2±0.8	23±2	56±18
	Not significant	Not significant	$P<0.01$	$P<0.01$

Confocal projections from three control and three *vps33b* IE18-injected 5 dpf larvae were altered as in Fig. 3E-J. Long ducts (blue) were counted and the length measured using a superimposed grid, and the numbers of interconnecting ducts (green) and terminal ductules (red) were also quantified. Numbers represent mean±s.d., and P values reflect t-test analysis.

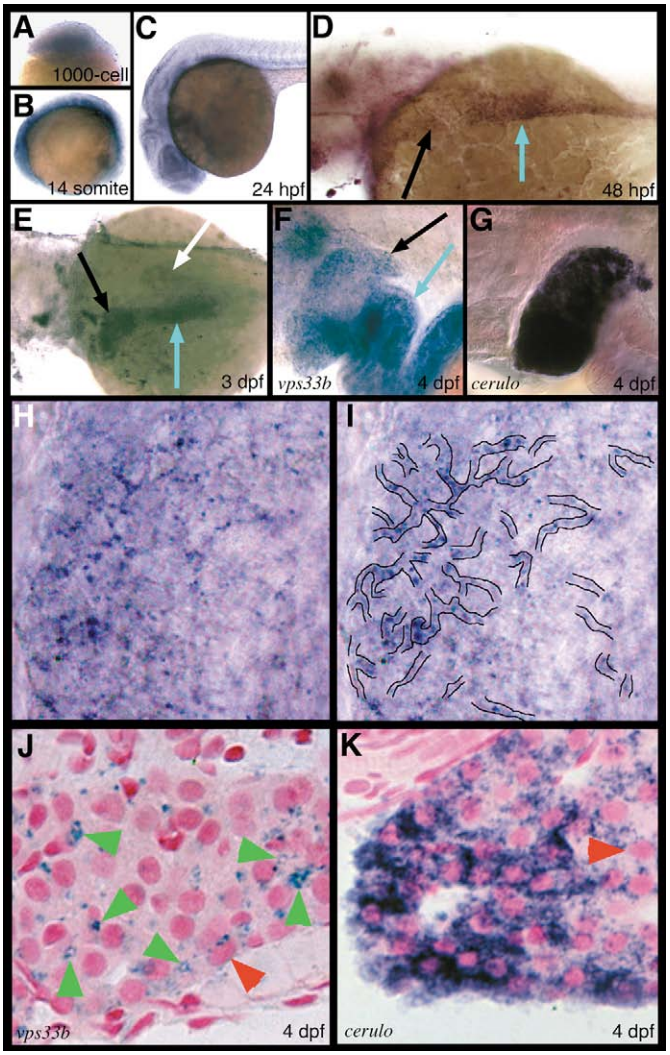

Fig. 2. *vps33b* expression in zebrafish embryos and larvae. (A-I) Whole-mount RNA in situ hybridization. Sphere stage (A), 10 somite (B) and 24 hpf (C) embryos show diffuse *vps33b* expression. (D) *vps33b* expression at 48 hpf is evident in the developing liver (black arrow) and proximal intestine (blue arrow). (E) Lateral view of a 72 hpf larva showing *vps33b* expression in the liver (black arrow) and proximal intestine (blue arrow). Weak pancreas expression (white arrow) is also evident. (F,G) High-power lateral views of 4 dpf larvae processed for *vps33b* and *ceruloplasmin* whole-mount RNA in situ hybridization. Liver (black arrow) demonstrates a reticular pattern of *vps33b* expression (black arrow) (F) compared with a homogeneous pattern of *ceruloplasmin* expression (G). Intestinal *vps33b* expression is also evident (blue arrow, F). (H) Higher power view of liver depicted in F. (I) Enhanced view of H outlining putative ducts. (J,K) Histological cross-sections of a 4 dpf larva processed for *vps33b* (J) and *ceruloplasmin* (K) whole-mount RNA in situ hybridization. These panels show punctate regions of *vps33b* expression in presumptive bile ducts (green arrowheads) and a small number of hepatocytes (red arrowheads). Biliary epithelial cell size and cytoplasm in these panels are comparable with biliary epithelial cell ultrastructure (Fig. 5) (Lorent et al., 2004; Matthews et al., 2004).

translational start site morpholino also had bile duct paucity (not shown), whereas injection with a missense IE18 control morpholino did not (not shown). Finally, co-injection of

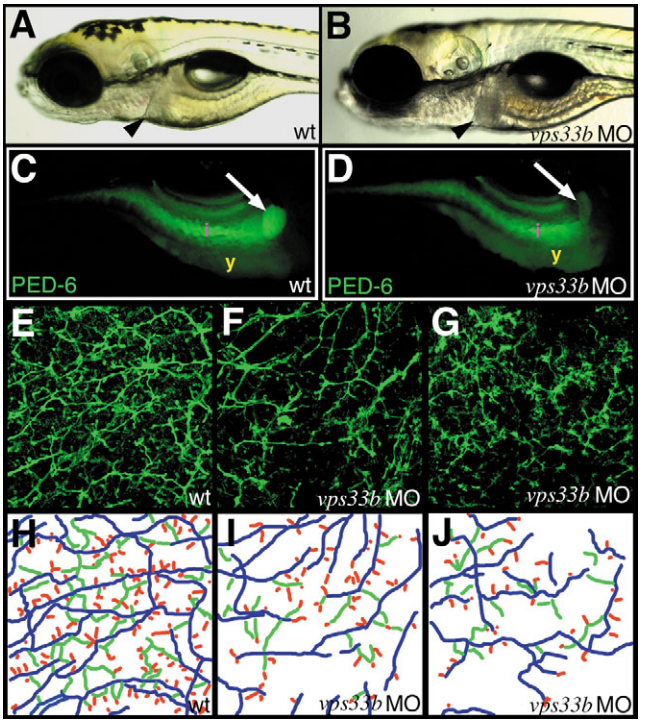

Fig. 3. *vps33b* knockdown disrupts zebrafish intrahepatic biliary development. (A,B) Left lateral views of 5 dpf wild-type (A) and *vps33b* (B) morpholino-injected larvae. Liver size (black arrowheads) is comparable in these larvae. (C,D) Right lateral fluorescent images of 6 dpf wild-type (C) and *vps33b* morpholino injected larvae (D) following ingestion of the PED-6 lipid reporter. Gallbladder fluorescence (white arrow) is decreased in morpholino-injected (D) larva relative to wild-type larva (C). i, intestinal fluorescence; y, endogenous yolk fluorescence. (E-G) Confocal projections through the liver of 5 dpf wild-type (E) and *vps33b* (F,G) larvae processed for keratin 18 immunohistochemistry. There are fewer bile ducts in F than in E; ducts are sparse, with fewer interconnecting ducts and terminal ductules. (H-J) Colorized schematics of bile ducts from E-G. Long ducts depicted in blue, interconnecting ducts in green and terminal ductules in red.

mRNA encoding zebrafish *vps33b* mRNA with the IE18 morpholino rescued biliary morphology (n=8 of 11 larvae analyzed; see Fig. S2 in the supplementary material). Taken together, these data strongly support a role for *vps33b* in zebrafish biliary development.

Normal motor axon and renal epithelial morphology in *vps33b*-deficient embryos

In contrast to the biliary defects present in the *vps33b*-deficient larvae, neither renal nor motor axon defects were identified. Motor axon anatomy of morpholino-injected larvae was analyzed using ZNP1 immunohistochemistry (n=300 hemisegments analyzed). Normal renal tubular epithelial cell morphology was confirmed histologically and using ultrastructural analyses (data not shown). Thus, we found no evidence that *vps33b* knockdown in zebrafish phenocopies the motor axon and renal defects associated with ARC.

One possible explanation for the lack of an effect in the spinal cord or kidney would be the presence of another *vps33*

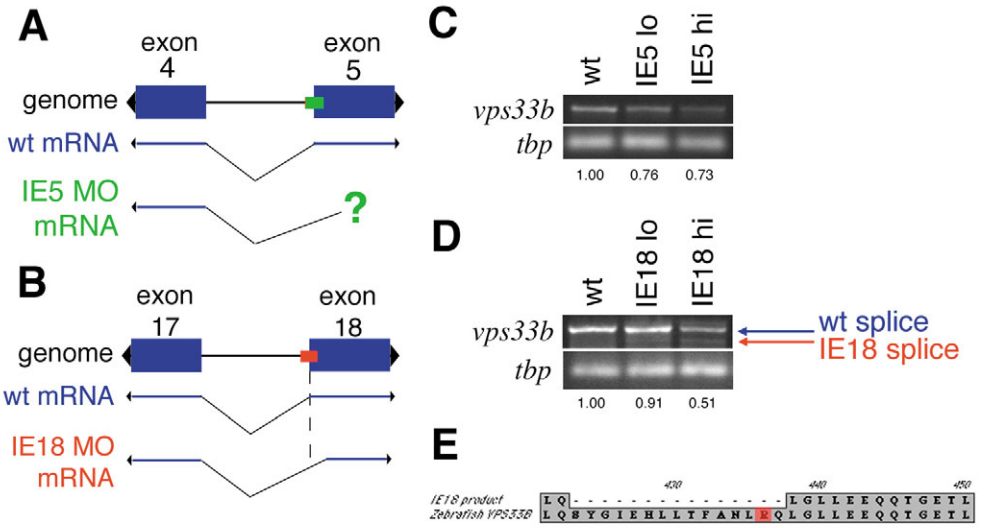

Fig. 4. *vps33b* morpholino targeting and altered splice product from IE18. (A,B) Schematics showing exons 4 and 5 and intervening intron 4 (A), and exons 17 and 18 and intervening intron 17 (B) of the *vps33b* gene. The sequences targeted by the IE5 and IE18 morpholinos are depicted in green and red, respectively. The wild-type and morpholino-targeted mRNA transcripts are depicted below the genomic region. Targeting by the IE18 morpholino generates a novel cDNA that uses a cryptic splice acceptor site within exon 18. The site of splicing induced by the IE5 morpholino could not be determined. (C,D) RT-PCR shows altered *vps33b* expression induced by both the IE5 and IE18 morpholinos. For these experiments, cDNA derived from 24 hpf wild-type and morpholino-injected larvae was amplified using primers flanking exons 5 or 18. There is decreased amplification of the wild-type *vps33b* fragment relative to *tbp*, quantified below, in both sets of morpholino-injected larvae. Wild-type (blue) and truncated (red) fragments are amplified from IE18 morpholino-injected larvae. (E) The shorter cDNA fragment amplified from IE18 morpholino injected larvae has an in-frame deletion of 15 amino acids includes R438 (red), which is mutated in some individuals with ARC.

paralog in the zebrafish genome. In mammals and insects, a second ortholog of yeast *vps33* has been identified. Mutation of this gene in the mouse (*buff*) alters coat pigmentation and platelet function (Suzuki et al., 2003), while mutation in the fly (*carnation*) alters eye pigmentation (Sevrioukov et al., 1999). We identified a zebrafish *vps33a* ortholog from the Ensembl database and generated morpholinos to the translation initiation site and the exon 4 splice acceptor site. An aberrant splice product of a 135 bp in-frame deletion was identified from EI4-injected 24 hpf embryos (data not shown). Knockdown of zebrafish *vps33a* did not disrupt motor neuron density (n=300 hemisegments), nor did it alter melanophore number or morphology (n=80 larvae examined; data not shown). Thus, *vps33a* does not perform the neuronal functions of *vps33b*, nor is it vital to pigmentation development. Of note, *vps33a* knockdown had no effect on biliary morphology (n=10 larvae examined; not shown). No other potential orthologs of *vps33b* were identified in the zebrafish genome assembly (Zv4).

Biliary and intestinal ultrastructural defects associated with *vps33b* knockdown

Class C VPS proteins, of which Vps33b is a member, function at multiple stages of intracellular transport in yeast and mammalian cells (Peterson and Emr, 2001; Kim et al., 2003; Richardson et al., 2004; Gissen et al., 2004). Mutation or overexpression of class C VPS genes disrupts cytoplasmic architecture, as manifest by the accumulation of cytoplasmic vesicles in affected cells. Ultrastructural analysis revealed cell-type specific defects in *vps33b* deficient zebrafish. In the liver, cytoplasmic vesicles were present within *vps33b* deficient biliary epithelial cells, whereas they were absent in the biliary cells of control larvae (Fig. 5A-B). These ultrastructural findings, which are nearly identical to those found with mutation of the yeast class C complex genes *vps18* (Rieder and Emr, 1997) and *vps11* (Peterson and Emr, 2001), suggest that bile duct paucity may arise autonomously in individuals with ARC from a defect in vesicle sorting.

We also examined intestinal ultrastructure in *vps33b* morpholino-injected larvae. As depicted in Fig. 6A-D, numerous vesicles and enlarged Golgi cisternae were seen in intestinal cells from *vps33b* morpholino larvae, but not in control larvae. This finding suggested disruption of the secretory pathway. Supporting this idea, intracellular vesicles accumulated in intestinal epithelial cells of *vps33b*-deficient larvae following ingestion of AM1-43, a fixable form of a

Table 3. Cell proliferation and death in *vps33b* morpholino-injected 4 dpf larvae

	Condition	Number of sections (number of larvae)	Number of cells examined	% positive (± s.d.)
PCNA	Wild type	8 (6)	692	93±7
	vps33b MO-injected	9 (8)	693	96±2
Apoptosis	Wild type	5 (7)	458	0
	vps33b MO-injected	5 (8)	432	0

Control and *vps33b*-injected 4 dpf larvae were assayed for cell proliferation using the proliferating cell nuclear antigen (PCNA) antibody marker or for cell death using the Apoptag system. Representative sections through livers of multiple larvae were counted for stained nuclei, demonstrating proliferation (PCNA) or cell death (Apoptag). Representative larvae (one or two) were assayed in each section, which accounts for the discrepancy between the number of sections and number of larvae. The difference between wild-type and *vps33b* MO-injected PCNA larvae is not significant.

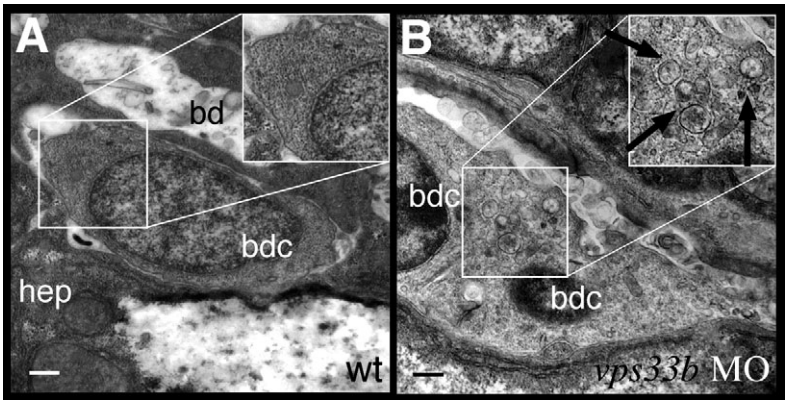

Fig. 5. *vps33b* knockdown disrupts biliary ultrastructure. (A,B) Electron micrographs of biliary epithelial cells from 5 dpf wild-type (A) and *vps33b* morpholino injected (B) larvae. The wild-type biliary cell cytoplasm has a homogeneous appearance. (B) A small bile duct comprising two bile duct cells from a *vps33b* morpholino-injected larva. Cytoplasm appears heterogeneously with multiple vesicles (black arrows). hep, hepatoctye; bd, bile duct lumen; bdc, bile duct cell.

styryl dye (FM1-43) used to track intracellular trafficking (Cochilla et al., 1999) (Table 4, Fig. 6E-H). Disruption of the secretory pathway could alter the uptake, intracellular transport or secretion of dietary lipids by enterocytes, and thus might underlie the malabsorptive diarrhea and poor growth frequently associated with ARC. Consistent with this idea, *vps33b*-deficient larvae fail to process doses of the PED-6 lipid reporter (see Fig. 3) that are readily processed by *hnf6*-deficient larvae with comparable biliary defects (Matthews et al., 2004).

Table 4. AM1-43 cell labeling

	Wild-type control	*vps33b* MO injected
Anterior intestine	1.05±0.39	1.80±0.46*
Posterior intestine	0.95±0.51	1.87±0.56*

Fluorescent vesicles were counted from mid and posterior intestine from three control and four *vps33b* morpholino-injected 6 dpf larvae in two separate sections, with ~75-100 cells/section, and normalized to the number of visible nuclei in each section. Anterior intestine is defined as intestine adjacent to the swim bladder. There is a ~1.8× increase in the morpholino injected larvae (*P<0.05). There is no difference between anterior and posterior intestine.

vps33b expression is dependent on *hnf6* activity

Biliary defects associated with *vps33b* knockdown were strikingly similar to the pattern we had previously observed in larvae injected with morpholino oligonucleotides directed against *hnf6* (Matthews et al., 2004). Quantitative real-time PCR experiments showed *vps33b* expression was reduced 75% in *hnf6*-deficient larvae relative to control larvae (Fig. 7; n=3 sets of independently derived morpholino-injected and control larvae; 15-20 larvae per morpholino and control pools). Whole-mount in situ hybridization confirmed a reduction in liver *vps33b* expression in these larvae, whereas expression of the hepatocyte marker *ceruloplasmin* in both quantitative PCR experiments and whole mount in situ hybridizations was unchanged (Fig. 7). *vps33b* expression was also reduced in larvae homozygous for a hypomorphic insertional mutation of

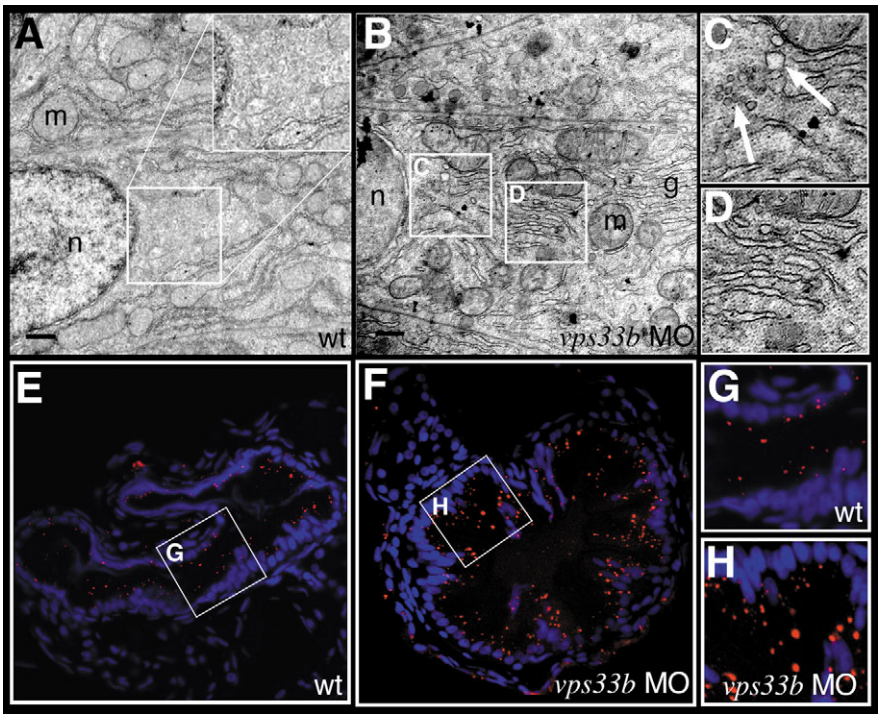

Fig. 6. *vps33b* knockdown disrupts intestinal vesicle transport. (A-D) Electron micrographs of enterocytes from 5 dpf wild-type (A) and *vps33b* morpholino injected (B-D) larvae. The apical surface is to the right of each panel. Insets are at twice the magnification of the indicated regions of cytoplasm. No vesicles can be identified within the wild-type cell cytoplasm. (C) Multiple vesicles (arrows) are seen in the cytoplasm of *vps33b*-deficient enterocyte. Dilated stacks of Golgi cisternae are also evident within these cells (D). g, golgi; m, mitochondria; n, nucleus. (E-H) Histological cross-sections from the anterior intestine of 5 dpf wild-type (E,G) and *vps33b* morpholino-injected (F,H) larvae that have ingested the styryl dye AM1-43. Nuclei stained with DAPI. (G,H) Magnified views from E and F, respectively. There was a 1.8-fold increase in the number of fluorescent vesicles in the *vps33b*-deficient larvae (see Table 4).

vhnf1 (Sun and Hopkins, 2002), a gene that is regulated by *hnf6* in zebrafish (Matthews et al., 2004) and mammals (Clotman et al., 2002) (Fig. 7). Conversely, injection of *vhnf1* mRNA doubled *vps33b* expression, while injection of *hnf6* mRNA increased *vps33b* expression by 30% (Fig. 7). These results support a model in which *hnf6*, functioning upstream of *vhnf1*, is required for basal expression of *vps33b*. Consistent with this model, *hnf6* morpholino injection results in a halving of *vps33b* expression in the hypomorphic *vhnf1* mutants (data not shown), presumably by knockdown of residual *vhnf1* activity.

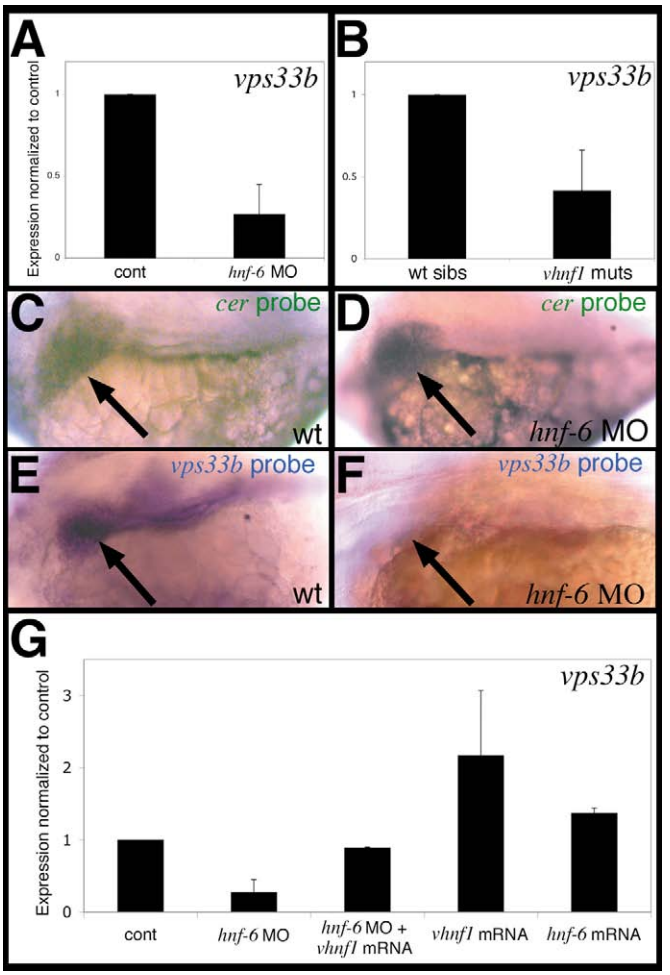

Fig. 7. *vps33b* expression is regulated by *hnf6/vhnf1*. (A,B) *vps33b* expression in 3 dpf wild-type (cont) *hnf6* morpholino-injected (A) and *vhnf1*mutant larvae (B) as determined by quantitative PCR. *vps33b* expression is reduced by 75% and 60%, respectively, in the *hnf6* morpholino-injected larvae and *vhnf1* mutants. Amplification levels normalized to wild type. (C-F) Whole-mount RNA in situ hybridization of 3 dpf wild-type (C,E) and *hnf6* (D,F) morpholino-injected larvae using a *ceruloplasmin* (C,D) or a *vps33b* (E-F) riboprobe. Liver (black arrows) *ceruloplasmin* expression is unchanged in the *hnf6* morpholino-injected larva, whereas decreased liver *vps33b* expression is evident. (G) Comparison of *vps33b* expression in 3 dpf wild-type larvae (cont) and in 3 dpf larvae injected with *hnf6* morpholino (*hnf6* MO), *hnf6* morpholino and *vhnf1*mRNA, *vhnf1* mRNA, or *hnf6* mRNA. These experiments are normalized to control expression and show decreased *vps33b* expression (by 75%, as above) in *hnf6*-deficient larvae that is restored with co-injection of *vhnf1* RNA. Microinjection of *vhnf1* on its own increases *vps33b* expression (2.2×), as does *hnf6* RNA to a lesser degree (1.3×). Error bars represent s.e.m. from six separate experiments.

Regulation of *vps33b* by *hnf6* and *vhnf1* suggests these genes may function in a common pathway during biliary development. This model predicts that partial knockdowns of *hnf6* and *vps33b* should act synergistically. Supporting this idea, biliary morphology was minimally disrupted in larvae injected with low doses of either the *hnf6* or *vps33b* morpholinos (predicted to only partially inhibit gene product translation; see Fig. S3 in the supplementary material), whereas bile duct paucity was present in compound morpholino-injected larvae (n=12) that was indistinguishable from paucity in larvae injected with standard doses of either the *vps33b* or *hnf6* morpholino (see Fig. S3 in the supplementary material). These results suggest that *hnf6* and *vps33b* function in a common genetic pathway that regulates bile duct formation, and are consistent with *hnf6* regulating *vps33b* expression, although they do not exclude the possibility that *hnf6* and *vps33b* function in parallel genetic pathways that each regulate biliary development.

Regulation of *vps33b* by *hnf6* and *vhnf1* through its target gene *vhnf1*

To further define the mechanism whereby *hnf6* and *vhnf1* regulate *vps33b* expression, we searched sequences within the *vps33b* promoter region for Hnf6 and vHnf1 binding sites. TESS-assisted (transcription element search system) and visual scanning of this sequence identified four putative Hnf1 sites and three Hnf6 sites (Fig. 8). To determine whether vHnf1 or Hnf6 regulated *vps33b* gene expression through binding at these sites, 1.5 kb of sequence immediately 5′ to the *vps33b* translation initiation start site was cloned into a luciferase reporter gene construct. This reporter construct was co-transfected with expression vectors for *hnf6* or *vhnf1* into mouse embryonic liver cells. Co-transfection of the *vps33b* reporter with the *vhnf1* expression vector stimulated reporter gene expression ~3.7 fold, while co-transfection with the *hnf6* expression vector had no significant effect (Fig. 8). Electrophoretic mobility shift assays demonstrated that the Hnf1-4 putative binding site binds vHnf1 protein, whereas Hnf6 was not bound by any of the putative binding sites within the *vps33b* promoter region (Fig. 8; data not shown). These data suggest that *hnf6* regulates *vps33b* expression indirectly, through *vhnf1*, and that *vhnf1*-mediated regulation likely occurs through direct binding of vHnf1 to the *vps33b* promoter. Interestingly, *vps33b* expression was reduced in *Hnf6*$^{-/-}$ mice only postnatally (see Fig. S4 in the supplementary material). These data suggest that the regulation of *vps33b* expression in mammals may be more complex than in zebrafish.

Discussion

The human ARC syndrome is one of several heritable disorders that present with cholestasis in infancy. The presence of bile duct paucity in liver biopsies of children with ARC suggests that cholestasis in this syndrome may arise from a primary defect of biliary development (Eastham et al., 2001). Here, we present data from the zebrafish that support this model. In addition, we identify defects in *vps33b* deficient intestinal epithelial cells that could account for the malabsorptive

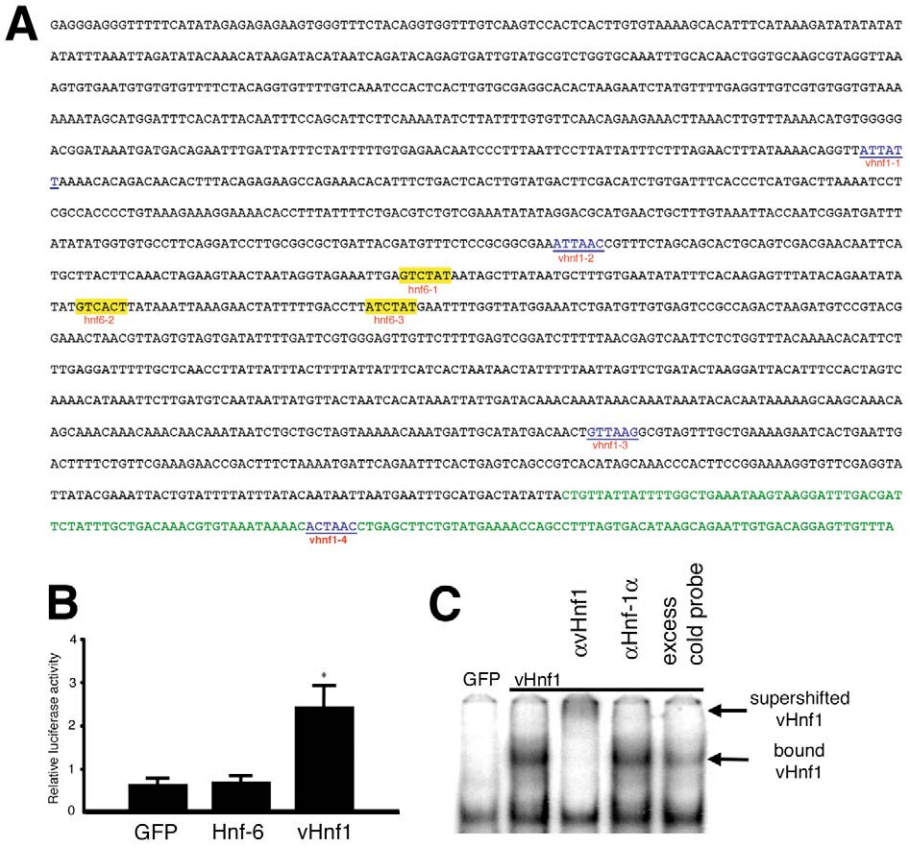

Fig. 8. Zebrafish *vps33b* promoter is regulated and bound by Hnf1. (A) Sequence of the putative zebrafish promoter. Predicted Hnf6 binding sites are highlighted in yellow, predicted vHnf1 binding sites are underlined and in blue, and the predicted sequence of the first untranslated exon is noted in green. (B) Expression of a luciferase *vps33b* reporter gene [*vps33b*(–1560/+139)-luciferase] is activated in BMEL cells by vHnf1, but not Hnf6 or GFP proteins. **P*<0.05. (C) Electrophoretic mobility shift assays performed using nuclear extracts from BMEL cells that were transfected with GFP (lane 1) or vHnf1 (lanes 2-5) expression constructs. Lanes in which the extracts are incubated with anti-vHnf1 antibody (vHnf1; lane 3), anti-Hnf-1α antibody (αHnf-1α; lane 4), or 50× excess cold probe directed against the vHnf1-4 site (lane 5) are noted. Addition of cold probe eliminates supershift seen in lane 3. Arrows indicates the gel shift resulting from vHnf1 binding (bound vHnf1) or vHnf1/anti-vHnf-1 antibody binding (supershifted vHnf1) to the labeled probe.

diarrhea and growth retardation seen in ARC. Finally, we present multiple lines of evidence suggesting that the *hnf6/vhnf1* pathway regulates *vps33b* expression in the developing zebrafish liver.

Knockdown of zebrafish *vps33b* phenocopies biliary defects in human ARC syndrome and ultrastructural defects associated with mutation of yeast class C vps genes

Analysis of pathological specimens from individuals with ARC has identified two possible mechanisms to account for cholestasis: bile duct paucity and altered bile secretion (Eastham et al., 2001). Either defect presents a plausible explanation for the development of cholestasis. Bile duct paucity, as occurs in Alagille syndrome, may lead to poor bile flow. Altered biliary secretion, such as occurs with mutation of hepatocyte canalicular transporters, causes cholestasis seen in the heritable human diseases collectively named progressive familial intrahepatic cholestasis (PFIC) syndromes.

Knockdown of zebrafish *vps33b* suggests that bile duct paucity is an important contributory factor to the pathogenesis of ARC liver disease. In all affected *vps33b* morpholino-injected larvae, the number of bile ducts was significantly reduced. Cytoplasmic inclusions reminiscent of the vesicular-like defects seen with yeast class C *vps* gene mutations were present in the biliary cells of *vps33b* morpholino-injected larvae. This finding, plus the selective pattern of *vps33b* expression within the larval zebrafish liver, suggests that biliary cells or committed biliary progenitors are targeted by loss of *vps33b* function. Alternative explanations for paucity, such as degeneration of biliary cells or failure of multipotent progenitors to adopt a biliary fate seem unlikely, as we saw no evidence of dying or degenerating biliary cells, nor did we see immature hybrid cells such as those seen in larvae injected with *jagged* morpholinos (Lorent et al., 2004).

Proteins encoded by class C vps genes form a complex in both mammals and yeast that is essential for intracellular protein trafficking (Rieder and Emr, 1997; Peterson and Emr, 2001; Kim et al., 2003). Mutations in yeast Class C *vps* genes are reported to interfere with Golgi-to-endosome and endosome-to-vacuole protein transport. Mammalian class C *vps* genes have been identified in both late and early endosomes, and bind to Golgi proteins (Kim et al., 2003; Richardson et al., 2004). Although we cannot precisely localize which component of the intracellular protein sorting pathway is disrupted in the *vps33b*-deficient biliary cells, we hypothesize it leads to the mislocalization or degradation of cellular proteins required for biliary epithelial cell development.

Intestinal epithelial defects in *vps33b*-deficient larvae

Although growth retardation is common in many cholestasis syndromes, severe fat malabsorption, such as occurs in ARC syndrome, is unusual. Here, we present several lines of evidence that knockdown of zebrafish *vps33b* phenocopies this feature of the ARC syndrome. First, Golgi abnormalities are present in the cytoplasm of *vps33b* morpholino-injected but not control intestinal epithelial cells. Second, *vps33b* morpholino-injected larvae fail to process conventional doses of PED-6, a

quenched fluorescent lipid that is absorbed in the intestine, that are normally processed by *hnf6*-deficient larvae with a comparable degree of bile duct paucity (Matthews et al., 2004). Third, labeling experiments using a fluorescent lipid (AM1-43) frequently used to track exocytosis (Cochilla et al., 1999) showed evidence of altered intestinal vesicle transport. These data suggest a model in which fat malabsorption arises from altered intracellular trafficking of dietary lipids within enterocytes. Although ultrastructural analysis of intestine from individuals with ARC has not been reported, we predict that defects related to those of *vps33b*-deficient zebrafish will be identified.

Disparity of the zebrafish *vps33b* knockdown and human ARC syndrome phenotypes

We found no evidence that *vps33b* knockdown generated the motoneuron defects responsible for congenital joint contractures (arthrogryposis) associated with ARC syndrome. This could be due to the existence of an unidentified *vps33b* paralogue, incomplete gene knockdown or a non-conserved role for *vps33b* in nervous system development. We believe the latter explanation is most likely. With respect to a possible additional paralogue, we have found only two *vps33* genes in zebrafish in silico, corresponding to *vps33a* and *vps33b*. Second, although the phenotype discrepancy could be due to incomplete gene knockdown (see below), we did not observe specific spinal neural expression of *vps33b*, suggesting that the function of *vps33b* in zebrafish spinal cord may be assumed by another gene. We did examine whether knockdown of zebrafish *vps33a* disrupted motoneuron development, but did not observe defects using either of two non-overlapping morpholinos. Cutaneous pigmentation was also normal in *vps33a*-deficient embryos, in contrast to coat hypopigmentation associated with mutation of mouse *vps33a* (Suzuki et al., 2003). Together, these findings suggest that the roles of Class C vps genes have evolved during vertebrate evolution. Interestingly, mutation of another zebrafish Class C vps gene, *vps18* (Golling et al., 2002), causes cutaneous hypopigmentation, hepatocyte defects and bile duct paucity, but neither motoneuron nor kidney defects (K. Sadler and N. Hopkins, personal communication). Overlapping biliary phenotypes of *vps33b*- and *vps18*-deficient larvae support the idea that zebrafish Class C proteins function in a complex, as described in yeast and mammals, while the difference in phenotypes suggests that there are cell-specific roles for the individual genes as well.

Kidney defects are another cardinal feature of the ARC syndrome. Several types of abnormalities have been described, including renal tubular epithelial degeneration, proximal renal tubular dysfunction (renal Fanconi syndrome), nephrocalcinosis and mis-sorting of apical proteins in kidney tubules (Nezelof et al., 1979; di Rocco et al., 1990; Horslen et al., 1994; Eastham et al., 2001; Gissen et al., 2004). Other than the absence of renal cell degeneration, we could not determine whether comparable kidney defects were present in *vps33b*-deficient larvae because we lack suitable markers and assays. A role for *vps33b* in zebrafish kidney seems unlikely, though, given the apparent lack of expression of *vps33b* expression in developing zebrafish glomerulus or pronephric duct of late embryos or larvae.

Partial loss-of-function or gene dose effects may be an alternative explanation for why motoneuron and renal defects were not identified in any of our *vps33b* morpholino-injected larvae. Although the amino acids deleted by the IE18 morpholino are contiguous with a binding motif essential for VPS33B function (Gissen et al., 2005), a significant percentage of *vps33b* transcripts were not efficiently targeted by either the IE18 or the IE5 morpholinos. Although there is currently no way of knowing whether the seemingly normal transcripts that persist in larvae injected with either of these morpholinos are translated in vivo, the data suggest that there is at least some residual *vps33b* activity in these fish. Consistent with this idea, a morpholino targeting the *vps33b* translation initiation codon was significantly more effective than either of the intron-exon morpholinos.

Regulation of *vps33b* by *hnf6* and *vhnf1*

Knockdown of zebrafish *vps33b* causes a paucity phenotype nearly identical to that associated with knockdown of *hnf6*. This, as well as several other pieces of evidence, supports the idea that *hnf6*, through its downstream target *vhnf1*, regulates *vps33b* expression in zebrafish. First, knockdown of *hnf6*, as well as mutation of *vhnf1*, reduces *vps33b* expression. Second, ectopic *vhnf1* expression, and to a lesser extent *hnf6* expression, increases endogenous *vps33b* expression in zebrafish embryos. Third, expression of zebrafish *vhnf1*, but not *hnf6,* in mammalian embryonic liver cells activates a zebrafish *vps33b* reporter construct, and vHnf1 binds a putative binding site within the *vps33b* promoter. Fourth, partial knockdowns of *hnf6* and *vps33b* act synergistically to disrupt biliary development. These data strongly support the idea that *vps33b* is a target of Hnf6/vHnf1 signaling.

Our data suggest that *vps33b* is not the only essential target of Hnf6/Hnf1 signaling required for biliary development. The cytoplasmic vesicles seen in the *vps33b* deficient biliary cells were not present in the biliary epithelial cells of *hnf6* morpholino-injected larvae. In addition, *vps33b* mRNA injections did not rescue *hnf6*-deficient larvae (R.P.M. and M.P., unpublished). We speculate that altered expression of other zebrafish *hnf6* target genes accounts for these findings. What role *hnf6*-directed expression of *vps33b* or other class C VPS genes plays during mammalian biliary development is uncertain. Our data show that *vps33b* expression was reduced in *hnf6* mutants on post-natal day 3, but not during embryonic stages. To account for these findings, we speculate that another class C VPS gene may function downstream of *hnf6* during bile duct development. Consistent with this idea, bile duct paucity has recently been reported in zebrafish *vps18* mutant larvae, although vesicle accumulation in hepatocytes, not bile duct cells, is reported in these mutants (Sadler et al., 2005).

The role of *vps33b* in biliary development

Knockdown of *vps33b* affects late stages of biliary development in zebrafish larvae, as reflected in the reduction of interconnecting and terminal ducts. Currently, the mechanism underlying expansion of the larval zebrafish biliary system is not known. We speculate that *vps33b* and possibly other Class C vps genes may play a role in either the differentiation of biliary progenitors or the growth of established biliary cells. Low-level apoptosis of biliary progenitors beyond the level we could detect with our assays, or non-apoptotic cell death of biliary cells, are alternative

explanations. The finding that *vps33b* knockdown leads to ultrastructural defects in existing biliary cells could be interpreted as supporting any of these mechanisms. Further experimentation will be required to distinguish between these possible mechanisms, each of which could arise from altered trafficking of membrane or secreted proteins.

The importance of *vps33b* in biliary development lies in the identification of proteins whose trafficking is dependent upon the function of class C vps genes. Proteins not properly localized to the cell membrane may include signaling receptors or ligands, as well as transporters that may function in biliary progenitors or other cell types. There may also be non-membrane cytoplasmic proteins that require the C complex for proper intracellular localization. Numerous human cholestatic conditions exist in which there are defects in members of these classes of proteins. Haploinsufficiency of the Notch ligand JAGGED1 causes Alagille syndrome, a developmental disorder of which bile duct paucity is a cardinal feature (Kamath and Piccoli, 2003). Mutations of genes required for bile secretion, such as the ABC superfamily members *FIC1*, *BSEP*, *MDR3* and *MRP2* cause chronic cholestasis in various PFIC syndromes (Tomer and Shneider, 2003). Finally, cystic fibrosis and α1-antitrypsin deficiency, both of which can be associated with cholestasis, result from mislocalization of their respective gene products. Whether mislocalization of these or other proteins in either hepatocyte or biliary cells leads to bile duct paucity or contributes to cholestasis in individuals with ARC is not known. Further knockdown experiments in zebrafish may help address this question.

We thank Wei-Long Gong and Erin Smith for expert technical assistance, Dr Daniel Kessler for use of his real-time PCR machine, Mark Paulosky for technical assistance with electron microscopy, and Dr Pierre Russo for discussion of electron micrographs. We also thank Dr Christopher Burd for helpful discussions. This work was supported by NIH grants RO-1 DK60369 (M.P.), T32 HD43021 and K08 DK68009 (R.P.M.); the Fred and Suzanne Biesecker Pediatric Liver Center at The Children's Hospital of Philadelphia; the Belgian State Program on Interuniversity Poles of Attraction; the DG Higher Education and Scientific Research of the French Community of Belgium; and the Fund for Scientific Medical Research (Belgium) (F.L.).

Supplementary material

Supplementary material for this article is available at
http://dev.biologists.org/cgi/content/full/132/23/5295/DC1

References

Clotman, F., Lannoy, V. J., Reber, M., Cereghini, S., Cassiman, D., Jacquemin, P., Roskams, T., Rousseau, G. G. and Lemaigre, F. P. (2002). The onecut transcription factor HNF6 is required for normal development of the biliary tract. *Development* **129**, 1819-1828.

Cochilla, A. J., Angleson, J. K. and Betz, W. J. (1999). Monitoring secretory membrane with FM1-43 fluorescence. *Annu. Rev. Neurosci.* **22**, 1-10.

Di Rocco, M., Reboa, E., Barabino, A., Larnaout, A., Canepa, M., Savioli, C. and Cremonte, M. (1990). Arthrogryposis, cholestatic pigmentary liver disease and renal dysfunction: report of a second family. *Am. J. Med. Genet.* **37**, 237-240.

Eastham, K. M., McKiernan, P. J., Milford, D. V., Ramani, P., Wyllie, J., van't Hoff, W., Lynch, S. A. and Morris, A. A. M. (2001). ARC syndrome: an expanding range of phenotypes. *Arch. Dis. Child* **85**, 415-420.

Farber, S. A., Pack, M., Ho, S. Y., Johnson, I. D., Wagner, D. S., Dosch, R., Mullins, M. C., Hendrickson, H. S., Hendrickson, E. K. and Halpern, M. E. (2001). Genetic analysis of digestive physiology using fluorescent phospholipid reporters. *Science* **292**, 1385-1388.

Gissen, P., Johnson, C. A., Morgan, N. V., Stapelbroek, J. M., Forshew, T., Cooper, W. N., McKiernan, P. J., Klomp, L. W., Morris, A. A., Wraith, J. E. et al. (2004). Mutations in VPS33B, encoding a regulator of SNARE-dependent membrane fusion, cause arthrogryposis-renal dysfunction-cholestasis (ARC) syndrome. *Nat. Genet.* **36**, 400-404.

Gissen, P., Johnson, C. A., Gentle, D., Hurst, L. D., Doherty, A. J., O'Kane, C. J., Kelly, D. A. and Maher, E. R. (2005). Comparitive evolutionary analysis of VPS33 homologues: genetic and functional insights. *Hum. Mol. Genet.* **14**, 1261-1270.

Golling, G., Amsterdam, A., Sun, Z., Antonelli, M., Maldonado, E., Chen, W., Burgess, S., Haldi, M., Artzt, K., Farrington, S. et al. (2002). Insertional mutagenesis in zebrafish rapidly identifies genes essential for early vertebrate development. *Nat. Genet.* **31**, 135-140.

Horslen, S. P., Quarrell, O. W. J. and Tanner, M. S. (1994). Liver histology in the arthrogryposis multiplex congenital, renal dysfunction, and cholestasis (ARC) syndrome: report of three new cases and review. *J. Med. Genet.* **31**, 62-64.

Huizing, M., Didier, A., Walenta, J., Anikster, Y., Gahl, W. A. and Krämer, H. (2001). Molecular cloning and characterization of human VPS18, VPS11, VPS16 and VPS33. *Gene* **264**, 241-247.

Johnson, C. A., Gissen, P. and Sergi, C. (2003). Molecular pathology and genetics of congenital hepatorenal fibrocystic syndromes. *J. Med. Genet.* **40**, 311-319.

Kamath, B. M. and Piccoli, D. A. (2003). Heritable disorders of the bile ducts. *Gastroenterol. Clin. N. Am.* **32**, 857-875.

Kay, A. R., Alfonso, A., Alford, S., Cline, H. T., Holgado, A. M., Sakmann, B., Snitsarev, V. A., Stricker, T. P., Takahashi, M. and Wu, L. G. (1999). Imaging synaptic activity in intact brain and slices with FM1-43 in C. elegans, lamprey, and rat. *Neuron* **24**, 809-817.

Kim, B. Y., Ueda, M., Kominami, E., Akagawa, K., Kohsaka, S. and Akazawa, C. (2003). Identification of mouse Vps16 and biochemical characterization of mammalian Class C Vps complex. *Biochem. Biophys. Res. Commun.* **311**, 577-582.

Lefebvre, J. L., Ono, F., Puglielli, C., Seidner, G., Franzini-Armstrong, C., Brehm, P. and Granato, M. (2004). Increased neuromuscular activity causes axonal defects and muscular degeneration. *Development* **131**, 2605-2618.

Lorent, K., Yeo, S.-Y., Oda, T., Chandrasekharappa, S., Chitnis, A., Matthews, R. P. and Pack, M. (2004). Inhibition of Jagged-mediated Notch signaling disrupts zebrafish biliary development and generates multi-organ defects compatible with an Alagille syndrome phenocopy. *Development* **131**, 5753-5766.

Matthews, R. P., Lorent, K., Russo, P. and Pack, M. (2004). The zebrafish onecut gene *hnf-6* functions in an evolutionarily conserved genetic pathway that regulates vertebrate biliary development. *Dev. Biol.* **274**, 254-259.

Nezelof, C., Dupart, M. C., Jaubert, F. and Eliachar, E. (1979). A lethal familial syndrome associating arthrogryposis multiplex congenita, renal dysfunction, and a cholestatic and pigmentary liver disease. *J. Pediatr.* **94**, 258-260.

Peterson, M. R. and Emr, S. D. (2001). The class C vps complex functions at multiple stages of the vacuolar transport pathway. *Traffic* **2**, 476-486.

Plumb-Rudewiez, N., Clotman, F., Strick-Marchand, H., Pierreux, C. E., Weiss, M. C., Rousseau, G. G. and Lemaigre, F. P. (2004). Transcription factor HNF-6/OC-1 inhibits the stimulation of the HNF-3alpha/Foxa1 gene by TGF-beta in mouse liver. *Hepatology* **40**, 1266-1274.

Richardson, S. C. W., Winistorfer, S. C., Poupon, V., Luzio, J. P. and Piper, R. C. (2004). Mammalian late vacuole protein sorting orthologues participate in early endosome fusion and interact with the cytoskeleton. *Mol. Biol. Cell* **15**, 1197-1210.

Rieder, S. E. and Emr, S. D. (1997). A novel RING finger protein complex essential for a late step in protein transport to the yeast vacuole. *Mol. Biol. Cell* **8**, 2307-2327.

Sadler, K. C., Amsterdam, A., Soroka, C., Boyer, J. and Hopkins, N. (2005). A genetic screen in zebrafish identifies the mutants *vps18*, *nf2*, and *foie gras* as models of liver disease. *Development* **132**, 3561-3572.

Sato, T. K., Rehling, P., Peterson, M. R. and Emr, S. D. (2000). Class C Vps protein complex regulates vacuolar SNARE pairing and is required for vesicle docking/fusion. *Mol. Cell.* **6**, 661-671.

Sevrioukov, E. A., He, J. P., Moghrabi, N., Sunio, A. and Kramer, H. (1999). A role for the deep orange and carnation eye color genes in lysosomal delivery in Drosophila. *Mol. Cell.* **4**, 479-486.

Sun, Z. and Hopkins, N. (2001). vhnf1, the MODY5 and familial GCKD-associated gene, regulates regional specification of the zebrafish gut, pronephros, and hiindbrain. *Genes Dev.* **15**, 3217-3229.

Suzuki, T., Oiso, N., Gautam, R., Novak, E. K., Panthier, J. J., Suprabha, P. G., Vida, T., Swank, R. T. and Spritz, R. A. (2003). The mouse organellar biogenesis mutant buff results from a mutation in Vps33a, a homologue of yeast vps33 and Drosophila carnation. *Proc. Natl. Acad. Sci. USA* **100**, 1146-1150.

Tomer, G. and Shneider, B. L. (2003). Disorders of bile formation and biliary transport. *Gastroenterol. Clin. N. Am.* **32**, 839-855.

Wallace, K. N. and Pack, M. (2003). Unique and conserved aspects of gut development in zebrafish. *Dev. Biol.* **255**, 12-29.